Baltic Astronomy, vol. 14, 495–510, 2005.

WASHINGTON PHOTOMETRY OF RED GIANTS IN FIVE GALACTIC GLOBULAR CLUSTERS

J. J. Clariá, M. C. Torres and A. V. Ahumada

Observatorio Astronómico, Universidad Nacional de Córdoba, Laprida 854, 5000 Córdoba, Argentina

Received 2005 April 12

Abstract. Surface metal abundances and effective temperatures of 165 stars in the Galactic globular clusters NGC 288, NGC 6397, NGC 6656, NGC 7078 and NGC 7089 are determined from photoelectric photometry in the *Washington* system. Mean cluster metal abundances are determined by the two-color diagram (TCD) technique described by Geisler et al. (1991). The resulting metallicities are compared with those derived by the standard giant branches (SGBs) method developed by Geisler and Sarajedini (1999). Although both methods provide metallicities in reasonably good agreement, we find that the SGBs technique yields metallicities in a better agreement with the existing metallicity scales. This is due to the higher metallicity sensitivity of the SGBs method as well as to its lower sensitivity to reddening and photometric errors.

Key words: methods: observational – techniques: photometric: Washington system – globular clusters – metal abundances

1. INTRODUCTION

Globular clusters are among the oldest known objects in our Galaxy and, for this reason, knowledge of their metal abundances is important to reconstruct chemical history of the Galactic halo. Without information about metallicities of these objects there is no possibility to determine their ages and investigate chemical evolution of the Galaxy. Accurate knowledge of the ages and chemical composition of globular clusters is also of vital importance for cosmology. The ages of globular clusters define the lower limit for the age of the Universe and the maximum limit of the Hubble constant. On the other hand, chemical composition of globular clusters, especially – the halo clusters, reveals the composition of the original matter prevalent in the earliest stages of the Galaxy.

Metallicity determinations of globular clusters usually are based on: (1) the integrated properties (integrated spectra and/or color indices), (2) morphological features of their color-magnitude diagrams, and (3) photometry or spectroscopy of individual giants. Although there are some inconsistencies among abundances derived by different methods (see, e.g., Nelles & Seggewiss 1984), the results based on photometry of individual giants seem to have a reasonable reliability. In particular, the *Washington* broad-band photometric system (Canterna 1976; Geisler 1986a) has proved to be very useful for metallicity determination in red giants (see, e.g., Geisler et al. 1991, hereafter GCM) using both traditional photoelectric photometry and CCD photometry with relatively small aperture telescopes. GCM

present an improved metal abundance calibration down to [Fe/H] $\approx$ –3, using high resolution spectroscopic abundances.

More recently, Geisler & Sarajedini (1999, hereafter GS) obtained CCD photometry in the *Washington* system C and T_1 filters for a very large sample of stars in ten globular clusters and in two old open clusters. Then, they constructed standard giant branches (SGBs) for these clusters in the absolute magnitude M_{T_1} vs. dereddened color $(C - T_1)_0$ plane. They derived metallicity calibrations for the $(C - T_1)_0$ color at three different fiducial M_{T1} values and for three different metallicity scales. They found that their SGBs method is much more metallicity sensitive than the two-color diagram (TCD) technique developed by GCM.

Here we report photoelectric observations in the *Washington* C, M, T_1 and T_2 filters for a large sample of suspected giants associated with five globular clusters – NGC 288, NGC 6397, NGC 6656 (M22), NGC 7078 (M15) and NGC 7089 (M2). All these clusters have metallicity estimates on the Zinn (1985) scale, which indicates that they are metal-poor or of intermediate metallicity, with –1.4 $\geq$ [Fe/H] $>$ –2.2. The clusters are quite loose, with low central concentration. This property facilitates the use of photoelectric aperture photometry. NGC 6397 and NGC 7078 have been used as prototypical metal-poor clusters by Da Costa & Armandroff (1990) and GS.

Our main goal is to determine abundances for these five globular clusters using the two above mentioned methods, and to compare the results obtained. These observations are described and the results presented in Section 2. In Section 3 we describe the derivation of physical parameters – luminosity classes, effective temperatures and surface metal abundances. In Section 4, we compare our own mean cluster metallicity values derived from both the TCD and SGBs methods.

2. OBSERVATIONS AND REDUCTIONS

Observations of 175 red giant candidates in the five globular clusters were obtained with the 1 m telescope at the Cerro Tololo Inter-American Observatory (CTIO) during seven mostly dark nights in July of 1990. A single-channel photometer was used in conjunction with a dry-ice-cooled Hamamatsu R943-02 GaAs photomultiplier. Pulse counting electronics and one of the standard *Washington* system C, M, T_1, T_2 filter sets (Geisler 1984) were used for all measurements.

All the stars observed in NGC 6656, NGC 7078 and NGC 7089 are cluster members according to previous proper motion studies carried out by Cudworth (1986), Cudworth (1976) and Cudworth & Rausher (1987), respectively. Since no proper motion study has been published for NGC 288 and NGC 6397, most of the stars in these two clusters were observed with the *DDO 51* filter. This filter measuring the Mg I triplet lines and a MgH band was first introduced in the *Vilnius* photometric system (Straižys & Zdanavičius 1965; Straižys 1977, 1992). Later on it was included into the *DDO* system by Clark & McClure (1979) and into the *Washington* system by Geisler (1984). A strong sensitivity of the Mg I triplet and MgH band on the surface gravity allows the *Washington* system to easily discriminate between dwarfs and giants of late G subclasses and all K subclasses.

The observations and reductions took place along the line described by Geisler (1986b). Diaphragm diameters for the program stars ranged from 11″ to 16″, depending on crowding and seeing, which was usually between 1″ and 2″. Mean extinction coefficients for CTIO were used in the reductions. Our intent was to

obtain a minimum of two independent observations of each cluster star in C, M, T_1 and T_2, as well as at least one observation in the *51* filter. The separation between dwarfs and giants in *M–51* at a given T_1–T_2 is of the order of 0.1–0.2 mag for G and K stars (Geisler 1984); hence, a high precision of $M-51$ is not required. The transformation to the standard *Washington* system was accomplished by observing each night 14 to 18 standard stars from the lists of Canterna (1976), Harris & Canterna (1979), Clariá & Lapasset (1985) and Geisler (1990). Nightly errors for the standards range between 0.01 and 0.02 mag.

The resulting mean colors and magnitudes for the program stars are presented in Table 1. The sources for star identifications are given at the end of the Table. Typical internal mean errors are 0.03, 0.01, 0.02, 0.03 and 0.02 mag for $C-M$, $M-T_1$, T_1-T_2, $M-51$ and T_1, respectively. All these errors are nearly similar to those obtained in previous papers (e.g., Geisler et al. 1992a) and should permit derivation of abundances with a precision of ~ 0.15 dex for intermediate metallicity cluster giants.

3. ANALYSIS

3.1. Interstellar reddening

As shown by GCM, the metallicity determination from *Washington* photometry largely depends on accurate account of the interstellar reddening. For cool, metal-poor giants, which represent an important fraction of the current star sample, the reddening is crucial. Reddening enters into the luminosity classification to a very small degree by its effect on the T_1-T_2 index. Increasing the reddening by an amount equal to its typical uncertainty ($\Delta E_{B-V} \approx 0.03$) will increase $T_{\rm eff}$ by $\sim$90 K (Geisler et al. 1992b). The same reddening uncertainty leads to an error in the derived metallicity for a giant with [Fe/H] = –1.5 from 0.2 to 0.4 dex depending, to a great extent, on the temperature of the star, and to a lesser extent, on the filters used to determine the metallicity (see GCM). For metal-poor giants with $(T_1-T_2)_0 < 0.57$ ($T_{\rm eff} > 4750$ K), reddening sensitivity is minimal and constant, while for cooler stars reddening sensitivity increases in proportion to the decrease in temperature.

In the present study, we have adopted the mean E_{B-V} color excesses given by Harris (1996), since we believe they represent the most updated values so far. All the studied clusters have well determined reddening values. The adopted E_{B-V} color excesses are presented in the second column of Table 3. NGC 6656 is more heavily reddened than the other clusters; furthermore, evidence for differential reddening has been found in this cluster (Minniti et al. 1992). NGC 288 and NGC 7089 exhibit very low reddening values, while the remaining three clusters are affected by E_{B-V} values ranging from 0.10 to 0.18.

3.2. Luminosity classification

16 stars in NGC 288 and 51 stars in NGC 6397 were observed with the *DDO 51* filter in addition to the standard C, M, T_1, T_2 filters. We performed the analysis described in Geisler (1984), based on the $(M-51)_0$ vs. $(T_1-T_2)_0$ two-color diagram, to discriminate between dwarfs and giants. Only one star in the entire sample, I-274 in NGC 6397, was found to be a dwarf and discarded from the abundance analysis. The remaining stars exhibit $(M-51)_0$ and $(T_1-T_2)_0$ indices compatible with the giant stars; nevertheless, their cluster membership is not

Table 1. Observed magnitudes and colors.

Star	$C-M$	$M-T_1$	T_1-T_2	$M-51$	T_1	n
NGC 288						
I-194	1.436	0.953	0.658	0.010	12.559	2
I-179	0.879	0.697	0.541	0.049	13.932	3
I-213	1.645	1.043	0.701		12.363	2
I-231	1.277	0.889	0.602	0.010	13.101	2
I-251	1.131	0.826	0.620	–0.033	13.250	3
I-277	1.227	0.865	0.593	0.052	13.332	2
I-287	1.256	0.849	0.603	0.032	13.098	2
I-307	1.226	0.834	0.598	0.014	13.330	3
II-48	1.396	0.951	0.653	–0.010	12.857	2
II-56	0.759	0.655	0.510		14.075	2
II-63	0.678	0.644	0.459		13.871	3
II-70	1.201	0.847	0.602	–0.002	13.495	2
II-77	1.581	0.997	0.714	0.043	12.588	3
II-80	1.240	0.841	0.610	–0.015	13.540	2
II-83	0.415	0.691	0.478		14.217	2
II-96	1.821	1.133	0.774		12.130	2
II-103	0.961	0.741	0.532	0.102	14.246	3
II-115	0.978	0.739	0.548	0.019	14.341	2
II-118	0.907	0.693	0.514	0.034	14.354	2
II-131	0.944	0.767	0.538	–0.002	14.114	3
II-158	0.782	0.655	0.487	0.015	14.096	2
NGC 6397						
I-275	1.233	0.986	0.725	0.067	10.382	3
I-268	0.734	0.723	0.627	0.095	13.203	3
I-276	0.610	0.682	0.599	0.049	13.492	3
I-385	0.661	0.707	0.548		13.558	2
I-386	0.713	0.747	0.585	0.024	13.434	4
I-264	0.881	0.823	0.634	0.055	12.058	3
I-269	1.168	0.956	0.705	0.053	10.567	4
I-272	1.066	0.903	0.678	0.044	10.942	3
I-274	0.595	0.716	0.546	–0.258	13.809	2
I-387	0.732	0.743	0.575	0.042	12.952	4
I-288	1.078	0.926	0.678	0.060	10.848	3
I-382	0.696	0.759	0.613	–0.037	13.622	2
I-379	0.660	0.713	0.601	–0.018	14.064	2
I-373	0.673	0.757	0.552	0.041	13.802	2
I-393	0.655	0.717	0.590	0.043	12.928	2
I-394	0.541	0.677	0.528		13.853	3
I-369	0.593	0.674	0.542		13.456	2
I-361	1.023	0.887	0.666	0.046	11.191	2
I-324	0.593	0.716	0.555		13.417	3
I-362	0.666	0.749	0.561	0.057	13.804	3
I-365	0.751	0.763	0.581	0.042	12.519	3
I-366	1.343	1.020	0.739	0.051	10.050	3
I-372	0.621	0.718	0.559	0.041	13.607	2
I-371	0.676	0.713	0.585	0.024	13.734	4
I-352	0.868	0.816	0.618	0.017	12.125	2
I-353	0.765	0.784	0.619	0.053	12.698	2
I-354	0.755	0.765	0.580	0.013	13.065	3
I-355	0.627	0.703	0.592	0.028	13.946	3
I-343	1.096	0.918	0.684	0.055	10.910	3
I-345	0.854	0.823	0.613	0.045	11.994	3

Table 1. (continued)

Star	$C-M$	$M-T_1$	T_1-T_2	$M-51$	T_1	n
NGC 6397						
I-300	0.914	0.848	0.645		11.783	3
I-380	0.821	0.804	0.628	0.049	12.024	2
I-360	0.531	0.717	0.550		14.026	2
I-340	1.721	1.063	0.692		9.281	3
I-337	0.892	0.814	0.635	0.023	12.085	2
I-331	1.777	1.218	0.845		9.176	2
I-328	0.910	0.832	0.642	0.039	11.559	2
I-314	0.905	0.850	0.635	0.060	11.692	3
I-305	0.997	0.880	0.663	0.049	11.106	2
I-302	1.546	1.103	0.782	0.059	9.702	2
I-292	0.870	0.815	0.620	0.059	12.099	3
I-296	0.724	0.687	0.600		13.368	2
I-322	1.011	0.885	0.666		11.344	2
I-321	0.926	0.840	0.644		11.549	2
II-144	1.119	0.934	0.685	0.033	10.575	3
II-1	1.700	1.186	0.826		9.374	2
II-61	0.789	0.791	0.597	0.024	12.492	2
II-42	0.697	0.758	0.578	0.034	13.198	2
II-74	0.998	0.870	0.654	0.036	11.264	3
II-93	0.859	0.804	0.610	0.042	12.180	2
II-90	0.789	0.778	0.610	0.038	12.412	2
II-104	0.875	0.821	0.612	0.037	11.812	3
II-116	1.477	1.077	0.764	0.048	9.960	2
II-133	0.831	0.800	0.618	0.024	12.329	2
II-139	0.866	0.833	0.622	0.037	12.105	2
II-163	0.868	0.827	0.605	0.031	11.966	3
II-166	0.926	0.851	0.645	0.043	11.644	3
II-169	0.886	0.838	0.623	0.039	12.113	2
II-180	0.765	0.789	0.603	0.016	12.537	3
II-200	0.849	0.818	0.622	0.022	12.280	2
II-206	1.222	0.981	0.718	0.042	10.927	4
II-216	0.775	0.774	0.595	0.051	12.665	2
II-230	0.718	0.680	0.523		13.752	2
II-256	0.930	0.847	0.632	0.040	11.809	2
II-244	0.717	0.792	0.604		13.428	2
NGC 6656						
I-1	1.139	0.998	0.776		12.402	2
I-12	1.635	1.207	0.886		11.125	2
I-16	1.026	0.938	0.764		13.137	2
I-17	1.185	0.997	0.751		12.332	3
I-19	1.382	1.049	0.815		12.091	2
I-25	1.157	0.977	0.764		12.703	3
I-27	1.173	0.971	0.729		12.765	2
I-28	1.010	0.870	0.718		13.096	3
I-29	0.976	0.961	0.699		13.441	3
I-34	1.087	0.946	0.726		13.018	2
I-35	1.055	0.946	0.734		12.442	3
I-37	1.388	1.084	0.817		11.926	2
I-40	1.435	1.126	0.840		11.468	2
I-49	1.449	1.073	0.791		11.857	2
I-50	1.011	0.921	0.728		12.850	2
I-53	1.082	0.942	0.744		12.728	2

Table 1. (continued)

Star	$C-M$	$M-T_1$	T_1-T_2	$M-51$	T_1	n
NGC 6656						
I-57	1.094	0.934	0.775		13.384	2
I-62	1.101	0.982	0.759		13.377	2
I-75	1.119	0.939	0.719		13.060	2
I-86	1.494	1.152	0.872		11.564	2
I-92	0.927	0.907	0.693		13.464	2
I-102	1.331	1.035	0.790		12.105	3
II-6	1.532	1.116	0.808		11.865	2
II-7	0.994	0.931	0.704		13.097	2
II-18	1.341	1.051	0.787		11.745	2
II-22	1.212	0.989	0.777		12.452	2
II-29	1.056	0.941	0.713		13.210	2
II-33	1.071	0.949	0.750		13.292	2
II-40	1.069	0.925	0.695		13.512	2
II-61	1.432	1.125	0.822		11.660	3
II-69	1.165	0.911	0.802		13.305	2
III-46	1.211	1.024	0.776		12.131	2
III-59	1.698	1.123	0.798		11.527	2
III-94	1.117	0.965	0.740		12.612	2
III-112	0.970	0.924	0.718		12.949	2
III-119	1.135	0.994	0.763		12.980	2
III-132	1.205	1.036	0.801		12.767	2
III-188	1.325	1.032	0.769		11.609	2
NGC 7078						
319	1.335	0.974	0.689		12.797	3
33	0.915	0.797	0.595		13.581	2
38	0.964	0.838	0.636		13.807	2
51	0.982	0.851	0.614		13.567	3
302	0.965	0.879	0.624		13.614	3
260	0.894	0.826	0.595		13.680	3
44	0.872	0.774	0.596		14.128	3
8	0.822	0.819	0.516		14.449	3
187	1.018	0.838	0.601		13.830	3
248	1.331	1.008	0.708		12.231	4
420	1.010	0.824	0.559		13.803	3
494	0.737	0.765	0.590		14.076	4
438	1.065	0.889	0.635		13.521	3
570	1.087	0.870	0.660		13.272	3
505	1.129	0.885	0.659		12.972	3
378	0.688	0.783	0.524		14.429	2
369	0.787	0.776	0.529		14.285	3
371	0.796	0.742	0.539		13.985	3
462	1.006	0.853	0.601		13.563	3
434	0.998	0.845	0.589		13.598	2
437	1.114	0.886	0.635		13.235	3
P6	0.832	0.783	0.577		14.460	3
P13	0.944	0.832	0.596		13.758	3
S11	0.847	0.790	0.558		14.080	3
S36	0.869	0.805	0.575		13.890	3
S37	0.760	0.754	0.562		14.904	2
X5	1.094	0.783	0.527		13.196	3
X6	0.983	0.844	0.590		13.617	2
90	1.024	0.823	0.666		13.222	2

Table 1. (continued)

Star	$C-M$	$M-T_1$	T_1-T_2	$M-51$	T_1	n
NGC 7089						
I-23	1.453	0.945	0.692		13.035	2
I-43	1.114	0.836	0.561		13.857	2
I-44	1.005	0.774	0.577		13.657	2
I-47	1.239	0.876	0.610		13.311	2
I-77	1.239	0.899	0.647		13.558	3
II-10	0.944	0.763	0.573		13.516	2
II-30	1.327	0.907	0.642		13.288	2
II-31	1.416	0.950	0.682		12.775	2
II-33	1.013	0.855	0.584		13.373	2
II-59	1.639	1.054	0.728		12.600	3
II-69	1.560	1.051	0.728		12.375	2
III-15	1.097	0.817	0.562		13.936	2
III-19	1.380	0.940	0.666		13.058	2
III-20	1.017	0.776	0.567		13.965	2
III-34	1.220	0.858	0.623		13.483	2
III-55	1.463	1.040	0.706		12.422	3
III-68	0.889	0.756	0.575		13.911	3
IV-22	1.186	0.828	0.584		13.410	2
IV-76	1.223	0.855	0.612		13.498	2
IV-79	1.690	1.077	0.730		12.501	2

NOTES: star designations for NGC 288 are from Alcaino (1975), for NGC 6397 from Alcaino (1977a), for NGC 6656 from Alcaino (1977b), for NGC 7078 from Buonanno et al. (1983) and Sandage (1970) and for NGC 7089 from Arp (1955).

warranted due to the possible existence of field giants at a distance which roughly coincides with cluster distances.

3.3. Effective temperatures

The effective temperatures were determined for all stars including nonmembers, using the calibrations presented in Geisler et al. (1992b). For such determination, we used $\log g = 1.5$ and interpolated between the metallicity grids to the appropriate mean cluster metal abundance. The results are given in column 2 of Table 2. For the isolated case of the star falling outside the calibration, no effective temperature is furnished. As has been shown in Geisler et al. (1992b), these effective temperatures should be accurate within ± 100 K, even when the temperatures for the nonmember stars are likely to have larger errors, since their metallicity, gravity and reddening may be different. The derived effective temperatures should prove useful for future studies, either as input temperatures for model atmosphere analysis of high dispersion spectroscopy or in the construction of HR diagrams for the comparative analysis with theoretical giant branch models.

3.4. Metallicities

In GCM the calibration of metallicity and temperature sensitive indices of the *Washington* system has been published. Although we followed their recommendations, we have not used the unreddened $M-T_1$ vs. T_1-T_2 diagram due to its small sensitivity to abundances for [Fe/H] ≤ -1. As a temperature index, we have used $M-T_2$, since it has a much broader baseline and thus the larger range than

Table 2. Effective temperatures and abundance indices.

Star	$T_{\rm eff}$	$\Delta'(C-M)$	$\Delta'(C-T_1)$	Star	$T_{\rm eff}$	$\Delta'(C-M)$	$\Delta'(C-T_1)$
NGC 288							
I-194	4437	–0.247	–0.292	II-63	5364	–0.326	–0.349
I-179	4917	–0.318	–0.376	II-70	4652	–0.298	–0.343
I-213		–0.182	–0.222	II-77	4245	–0.223	–0.292
I-231	4652	–0.282	–0.312	II-80	4617	–0.262	–0.314
I-251	4575	–0.364	–0.428	II-83*		–0.683	–0.702
I-277	4691	–0.285	–0.318	II-103	4956	–0.286	–0.322
I-287	4647	–0.247	–0.292	II-115	4887	–0.289	–0.337
I-307	4669	–0.249	–0.295	II-118	5049	–0.246	–0.287
II-48	4455	–0.282	–0.321	II-131	4930	–0.349	–0.380
II-56	5072	–0.333	–0.386	II-158	5203	–0.278	–0.315
NGC 6397							
I-275	4628	–0.459	–0.515	I-328	4935	–0.443	–0.498
I-268	4991	–0.441	–0.525	I-314	4961	–0.463	–0.508
I-386	5220	–0.436	–0.485	I-305	4858	–0.454	–0.507
I-264	4965	–0.447	–0.501	I-302*	4428	–0.294	–0.334
I-269	4702	–0.452	–0.506	I-292	5025	–0.427	–0.474
I-272	4802	–0.440	–0.494	I-296	5136	–0.361	–0.440
I-387	5275	–0.397	–0.441	I-322	4847	–0.452	–0.505
I-288	4802	–0.461	–0.507	I-321	4928	–0.441	–0.495
I-382	5064	–0.511	–0.573	II-144	4776	–0.441	–0.489
I-379	5131	–0.464	–0.534	II-1*		–0.257	–0.286
I-373	5403	–0.443	–0.467	II-61	5153	–0.441	–0.481
I-393	5192	–0.459	–0.521	II-42	5259	–0.458	–0.498
I-361	4847	–0.443	–0.495	II-74	4890	–0.426	–0.476
I-362	5353	–0.452	–0.484	II-93	5081	–0.408	–0.452
I-365	5242	–0.416	–0.456	II-90	5081	–0.441	–0.494
I-366	4576	–0.380	–0.432	II-104	5070	–0.419	–0.459
I-371	5220	–0.425	–0.485	II-116*	4486	–0.322	–0.363
I-352	5036	–0.427	–0.473	II-133	5036	–0.441	–0.493
I-353	5031	–0.486	–0.544	II-139	5014	–0.459	–0.502
I-354	5148	–0.413	–0.452	II-163	5109	–0.424	–0.458
I-355	5181	–0.469	–0.538	II-166	4924	–0.458	–0.509
I-343	4780	–0.440	–0.493	II-169	5009	–0.448	–0.489
I-345	5064	–0.444	–0.484	II-180	5120	–0.470	–0.516
I-300	4924	–0.466	–0.518	II-200	5014	–0.455	–0.503
I-380	4987	–0.471	–0.528	II-206	4654	–0.453	–0.506
I-340*		0.002	–0.005	II-216	5164	–0.427	–0.473
I-337	4961	–0.425	–0.482	II-256	4972	–0.430	–0.474
I-331*		–0.228	–0.25	II-244	5114	–0.524	–0.569
NGC 6656							
I-1	4798	–0.449	–0.513	I-37	4646	–0.382	–0.443
I-12	4405	–0.390	–0.441	I-40	4561	–0.428	–0.489
I-16	4842	–0.459	–0.536	I-49*	4742	–0.268	–0.315
I-17	4891	–0.366	–0.414	I-50	4976	–0.399	–0.458
I-19	4653	–0.335	–0.406	I-53	4916	–0.380	–0.443
I-25	4842	–0.384	–0.447	I-57	4801	–0.401	–0.487
I-27	4972	–0.310	–0.352	I-62	4861	–0.440	–0.498
I-28	5019	–0.312	–0.383	I-75	5014	–0.303	–0.351
I-29	5125	–0.449	–0.476	I-86	4450	–0.409	–0.479
I-34	4983	–0.355	–0.405	I-92	5158	–0.419	–0.454
I-35	4953	–0.399	–0.453	I-102	4746	–0.300	–0.390

Table 2. (continued)

Star	$T_{\rm eff}$	$\Delta'(C-M)$	$\Delta'(C-T_1)$	Star	$T_{\rm eff}$	$\Delta'(C-M)$	$\Delta'(C-T_1)$
NGC 6656							
II-6*	4679	−0.271	−0.314	II-69	4702	−0.336	−0.447
II-7	5097	−0.396	−0.436	III-46	4798	−0.415	−0.469
II-18	4757	−0.339	−0.391	III-59*		−0.101	−0.135
II-22	4794	−0.365	−0.432	III-94	4931	−0.373	−0.424
II-29	5047	−0.361	−0.403	III-112	5019	−0.430	−0.481
II-33	4894	−0.410	−0.474	III-119	4846	−0.429	−0.486
II-40	5147	−0.299	−0.335	III-132	4705	−0.474	−0.540
II-61	4628	−0.404	−0.453	II-188	4824	−0.302	−0.349
NGC 7078							
319	4556	−0.360	−0.403	378	5251	−0.524	−0.531
33	4904	−0.418	−0.467	369	5223	−0.422	−0.435
38	4753	−0.487	−0.548	371	5158	−0.379	−0.410
51	4834	−0.456	−0.498	462	4882	−0.416	−0.449
180	5018	−0.446	−0.490	434	4927	−0.396	−0.424
302	4797	−0.527	−0.566	437	4756	−0.404	−0.448
260	4904	−0.481	−0.519	457	4964	−0.470	−0.523
44	4901	−0.430	−0.487	P6	4971	−0.456	−0.497
8	5296	−0.430	−0.419	P13	4901	−0.441	−0.478
187	4882	−0.383	−0.421	S11	5062	−0.423	−0.450
248	4488	−0.457	−0.509	S36	4979	−0.447	−0.480
420		−0.311	−0.326	S37	5040	−0.465	−0.507
494		−0.543	−0.600	X5*		−0.122	−0.131
438	4756	−0.457	−0.500	X6	4923	−0.411	−0.440
570	4664	−0.444	−0.509	90	4641	−0.448	−0.534
505	4667	−0.422	−0.482				
NGC 7089							
I-23	4273	−0.234	−0.301	II-69		−0.335	−0.385
I-43	4770	−0.274	−0.292	III-15	4770	−0.264	−0.288
I-44	4700	−0.317	−0.367	III-19	4361	−0.271	−0.321
I-47	4561	−0.276	−0.312	III-20	4744	−0.293	−0.336
I-77	4426	−0.362	−0.414	III-34	4514	−0.288	−0.339
II-10	4718	−0.356	−0.408	III-55	4225	−0.411	−0.443
II-30	4445	−0.251	−0.297	III-68		−0.404	−0.459
II-31	4307	−0.268	−0.326	IV-22	4670	−0.223	−0.259
II-33	4670	−0.435	−0.461	IV-76	4554	−0.265	−0.309
II-59		−0.222	−0.271	IV-79		−0.191	−0.230

Table 3. Mean abundances in the clusters.

NGC	E_{B-V}	$[\mathrm{Fe/H}]_{\rm TCD}$	N_1	$[\mathrm{Fe/H}]_{\rm SGB}$	N_2	$\lvert\Delta[\mathrm{Fe/H}]_{\rm SGB-Z}\rvert$	$\lvert\Delta[\mathrm{Fe/H}]_{\rm TCD-Z}\rvert$
288	0.03	−1.22 ± 0.05	19	−1.47 ± 0.03	16	0.07	0.18
6397	0.18	−2.15 ± 0.03	51	−1.94 ± 0.02	66	0.03	0.24
6656	0.34	−1.80 ± 0.05	35	−1.79 ± 0.04	29	0.04	0.05
7078	0.10	−2.09 ± 0.07	30	−2.12 ± 0.04	28	0.03	0.06
7089	0.06	−1.29 ± 0.07	20	−1.83 ± 0.03	16	0.21	0.33

$T_1 - T_2$; therefore, it is less sensitive to photometric errors. This temperature index is especially preferable for cool, metal-poor stars. To derive abundances by the TCD technique, we have used the $\Delta'(C-M)_{M-T_2}$ and $\Delta'(C-T_1)_{M-T_2}$ indices defined by GCM. The total sensitivity of these indices may be somewhat

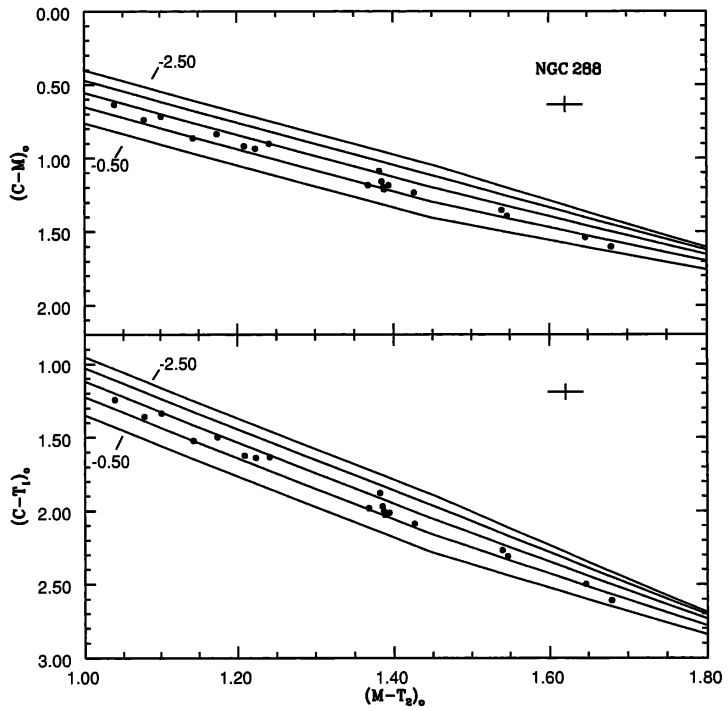

Fig. 1. Two-color diagrams of NGC 288 from which metallicities are derived. Typical error bars are shown in the upper right. The iso-abundance relations from GCM for 0.5 dex intervals in metallicity, labelled with representative [Fe/H] values are also given.

smaller than that of other indices; however, they do provide the smallest internal abundance dispersion when applied to metal-poor globular clusters.

Figures 1–5 show the dereddened $C-M$ vs. $M-T_2$ and $C-T_1$ vs. $M-T_2$ TCDs for the cluster members in each of the five studied clusters. Iso-abundance lines for 0.5 dex intervals from [Fe/H] = –0.5 to –2.5 are shown. Typical photometric errors are also presented.

For each observed star we determined the metallicity-sensitive $\Delta'(C-M)_{M-T_2}$ and $\Delta'(C-T_1)_{M-T_2}$ values as defined in GCM. These quantities are displayed in columns 3 and 4 of Table 2. A few stars (indicated by asterisks in Table 2), which appear to be giants from photometry, exhibit unreasonably high or low metallicities. These stars may be field stars, binaries or observed with lower accuracy. They have not been plotted in Figures 1–5. In order to determine the mean cluster metallicity, we first excluded all stars marked in Table 2 by asterisks and then derived the mean Δ' value for each index with equal weights. However, the abundances for stars with $(M-T_2)_0 > 1.45$ can be of lower accuracy. Finally, two different values of the iron-to-hydrogen ratio were derived from the expression:

$$[\mathrm{Fe/H}] = (-b + \sqrt{b^2 - 4a(c-\Delta')})/2a, \qquad (1)$$

where the constants a, b and c are given in GCM's Table 10. The resulting [Fe/H] values are given in column 3 of Table 3, together with the standard deviation of the mean $(\sigma/\sqrt{N_1})$ and the number N_1 of red giants finally used to derive the cluster metallicity.

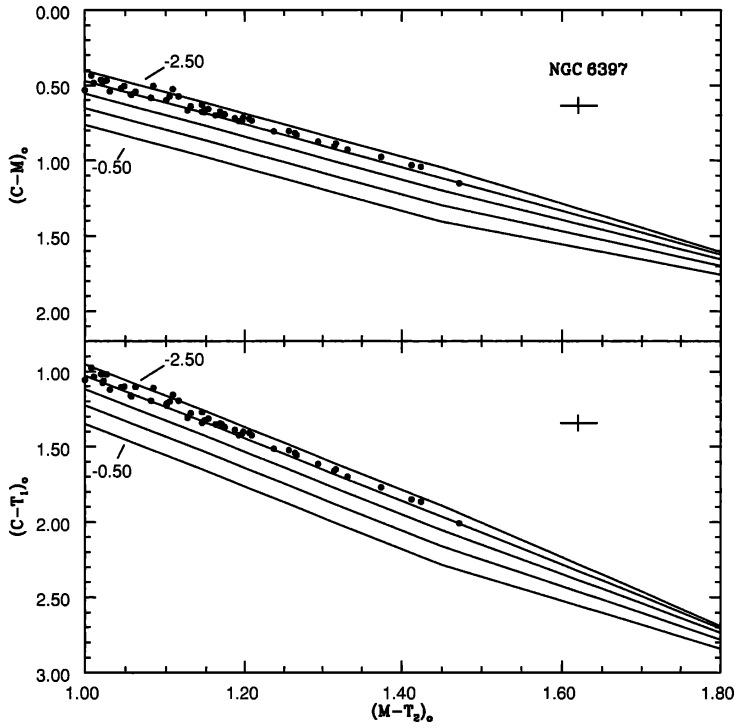

Fig. 2. Two-color diagrams of NGC 6397. For comments see Fig. 1.

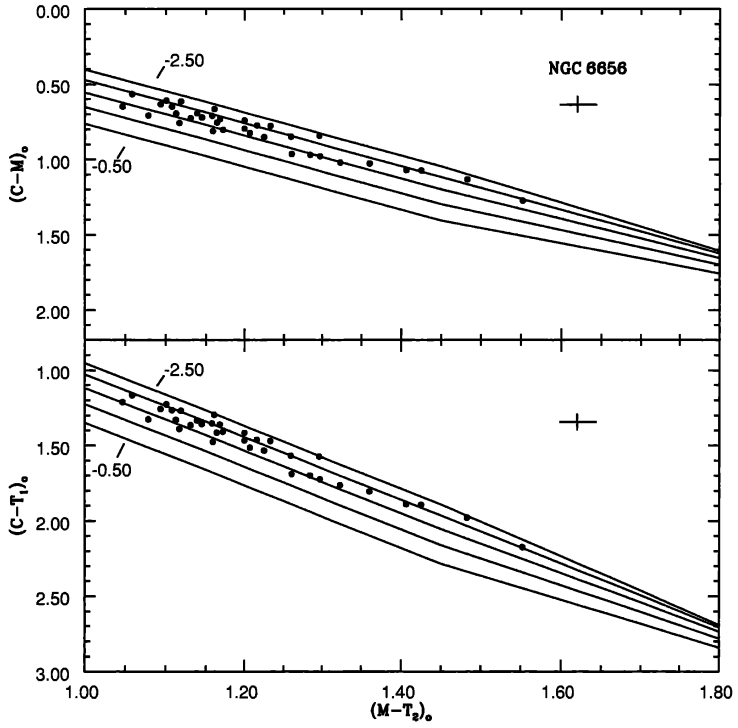

Fig. 3. Two-color diagrams of NGC 6656 (M 22). For comments see Fig. 1.

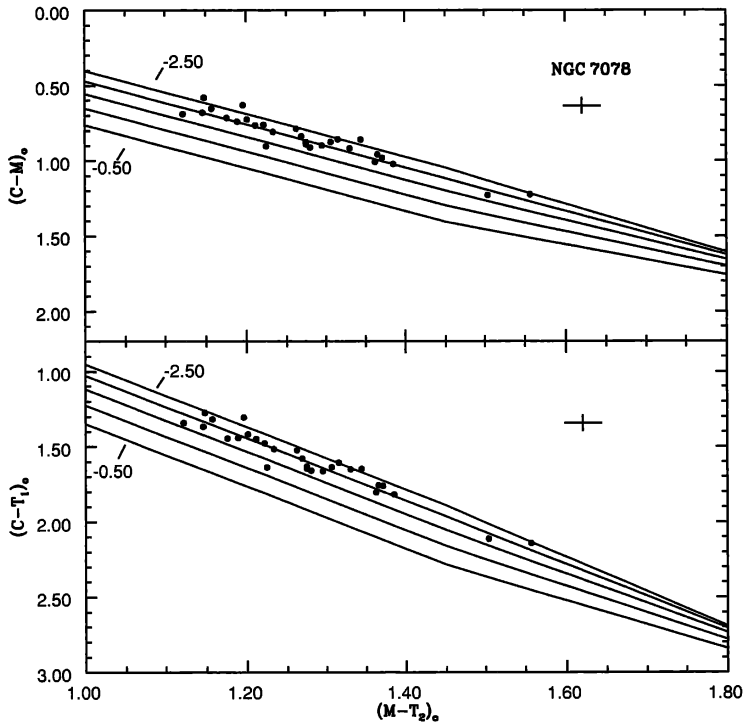

Fig. 4. Two-color diagrams of NGC 7078 (M 15). For comments see Fig. 1.

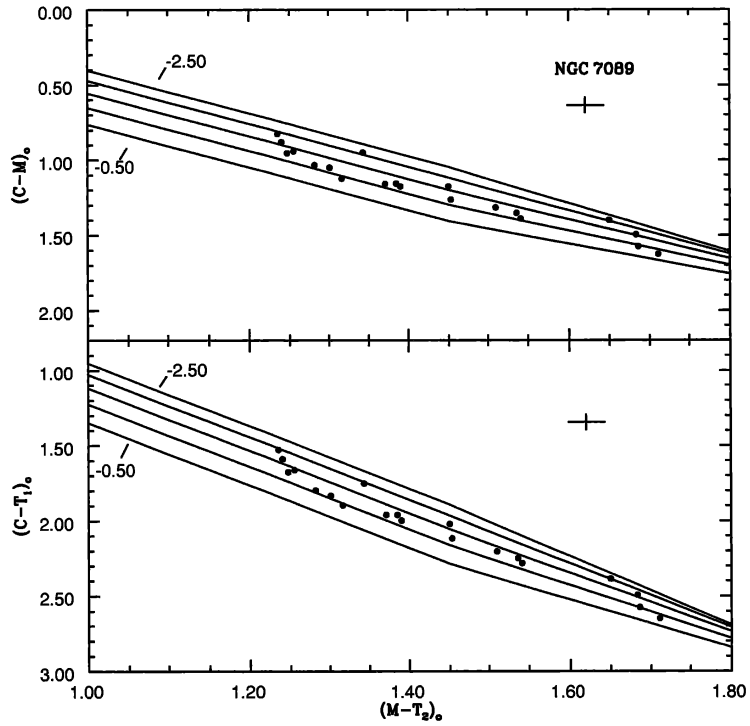

Fig. 5. Two-color diagrams of NGC 7089 (M2). For comments see Fig. 1.

Since the Standard Giant Branches (SGBs) technique developed by GS is particularly applicable to metal-poor globular cluster stars, we decided to apply this technique also to the five observed globular clusters in order to compare the results with those obtained by the TCD method. To transform the observational T_1 vs. $C-T_1$ plane to the absolute magnitude M_{T_1} vs. dereddened color $(C-T_1)_0$ plane, it is enough to take into account that:

$$M_{T_1} = T_1 - A_{T_1} - (V - M_V) + A_V, \tag{2}$$

where A_{T_1} and A_V represent the extinction in the T_1 and V passbands, respectively. By adopting the relations $A_V = 3.2E_{B-V}$ and $A_{T_1} = 2.62E_{B-V}$ obtained by Dean et al. (1978) and Geisler et al. (1996), respectively, we reach the following expression:

$$M_{T_1} = T_1 + 0.58E_{B-V} - (V - M_V). \tag{3}$$

Additionally, from the relation between color excesses in the *UBV* and *Washington* systems, we derive:

$$(C - T_1)_0 = (C - T_1) - 1.97E_{B-V}. \tag{4}$$

Equations (3) and (4) allow us to transform the M_{T_1} vs. $C - T_1$ plane into the M_{T_1} vs. $(C-T_1)_0$ plane, since the color excesses E_{B-V} and the apparent distance moduli of the clusters are already known.

Figures 6 to 10 show the M_{T_1} vs. $(C - T_1)_0$ diagrams obtained for the five globular clusters. The fits were performed using the IRAF routine CURFIT. In order to determine metallicities, the calibration corresponding to $M_{T_1} = -2.0$ and the metallicity scale from Zinn (1985, hereafter Z85) were adopted. The resulting metallicities are displayed in column 5 of Table 3, together with the estimated internal uncertainties and the number N_2 of red giants used.

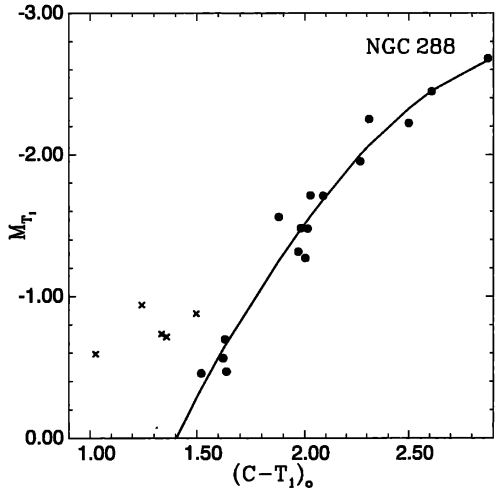

Fig. 6. The M_{T_1} vs. $(C - T_1)_0$ CMD for the NGC 288 stars. Filled circles are used in the fit.

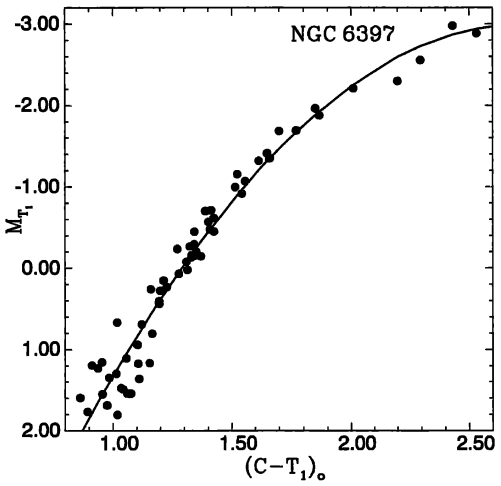

Fig. 7. The M_{T_1} vs. $(C-T_1)_0$ CMD for the NGC 6397 stars.

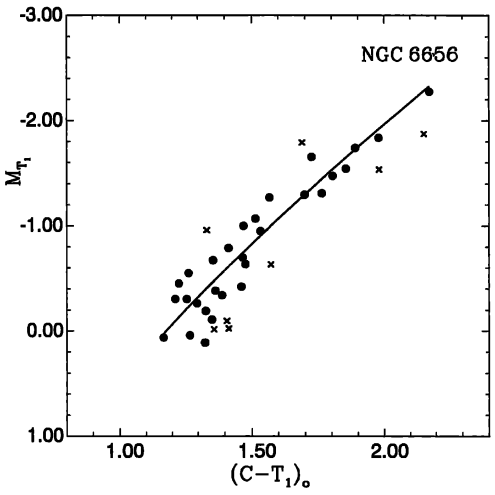

Fig. 8. The M_{T_1} vs. $(C-T_1)_0$ CMD for the NGC 6656 stars. Filled circles are used in the fit.

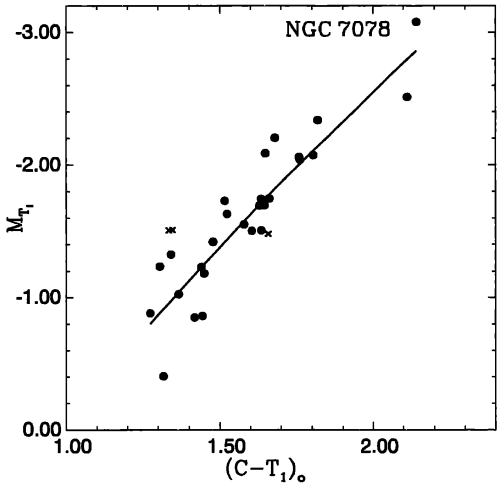

Fig. 9. The M_{T_1} vs. $(C-T_1)_0$ CMD for the NGC 7078 stars. Filled circles are used in the fit.

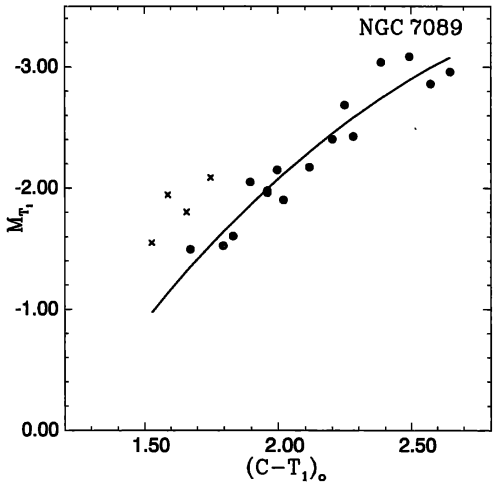

Fig. 10. The M_{T_1} vs. $(C-T_1)_0$ CMD for the NGC 7089 stars. Filled circles are used in the fit.

4. COMPARISON OF THE RESULTS

In columns 7 and 8 of Table 3 we present the difference (in absolute value) between the metallicities derived in the present study and those given in the widely accepted Z85 scale. The metallicities derived by the SGBs technique coincide very well with the corresponding Z85 values, the mean difference being $\mid \Delta[\mathrm{Fe/H}]_{\mathrm{SGB-Z}} \mid = 0.08 \pm 0.07$ (σ). On the contrary, the mean difference between the metallicities derived by the TCD method and those of the Z85 scale results in $\mid \Delta[\mathrm{Fe/H}]_{\mathrm{TCD-Z}} \mid = 0.17 \pm 0.10$ (σ), i.e., more than twice larger than the former mean difference. These results do not change if, instead of the Z85 scale, the Zinn & West (1984, hereafter ZW84) calibration is used. This fact can

be explained by different sensitivity of both methods to the interstellar reddening and photometric errors.

If instead of $M_{T_1} = -2.0$ we adopt the fiducial absolute magnitude M_{T_1} values –1.5 or –2.5, the corresponding mean difference $\mid \Delta[\mathrm{Fe/H}]_{\mathrm{SGB-Z}} \mid$ practically remains the same. As a matter of fact, quite independently from the adopted fiducial absolute magnitude, metallicities derived by the SGBs method turn out to be in the best agreement with the Z85 scale. The choice of the Z85 scale is not only due to the fact that it has been in vogue for many years and is widely accepted, but also because the five clusters studied in this work have [Fe/H] values available in this scale.

Based on their high-dispersion spectroscopic studies of a large number of globular cluster giants, Carretta & Gratton (1997, hereafter CG97) proposed a new metallicity scale, which is supported by the Ca II strengths measured by Rutledge et al. (1997). More recently, Kraft & Ivans (2003) derived another globular cluster metallicity scale, based on the equivalent widths of Fe II lines measured from high-dispersion spectra of giants in 16 selected clusters. Unfortunately, the clusters NGC 6656 and/or NGC 7089 are not included in these calibrations; thus, it is not possible to obtain the comparisons with our results. On the other hand, the metallicity assigned to NGC 288 by CG97, i.e., [Fe/H] = –1.07, is by 0.2–0.3 dex greater than the value obtained in several subsequent works (see, e.g., Davidge & Harris 1997; Shethrone & Keane 2000; Kraft & Ivans 2003). Taking for NGC 288 the value obtained recently by Kraft & Ivans (2003), i.e., [Fe/H] = –1.41, and the CG97 scale for the remaining three clusters (NGC 6397, NGC 6656 and NGC 7078), the following mean differences are found: $\mid \Delta[\mathrm{Fe/H}]_{\mathrm{SGB-CG}} \mid = 0.12 \pm 0.11$ and $\mid \Delta[\mathrm{Fe/H}]_{\mathrm{TCD-CG}} \mid = 0.22 \pm 0.11$, which still support the former conclusion. Table 4 displays the [Fe/H] values for the five globular clusters derived here by the SGBs method compared with the results obtained earlier.

Table 4. Mean metallicities for globular clusters compared to the literature data.

NGC	$[\mathrm{Fe/H}]_{\mathrm{SGB}}$	AZ88	CD88	M93	CG97	RHR99	H03	KI03
288	–1.47		–1.00		–1.07		–1.24	–1.41
6397	–1.94		–1.85	–1.99	–1.82		–1.95	–2.02
6656	–1.79				–1.48	–1.62	–1.64	
7078	–2.12	–2.17		–2.23	–2.12		–2.26	–2.42
7089	–1.83	–1.58					–1.62	

References: AZ88 (Armandroff & Zinn 1988), CD88 (Caldwell & Dickens 1988), M93 (Minniti et al. 1993), CG97 (Carretta & Gratton 1997), RHR99 (Richter et al. 1999), H03 (Harris 2003), KI03 (Kraft & Ivans (2003).

ACKNOWLEDGMENTS. We are gratefully indebted to the CTIO staff members and night assistants for their kind hospitality and support during the observing run. This work was supported by the Argentinian institutions CONICET, Agencia Nacional de Promoción Científica y Tecnológica (ANPCyT) and Agencia Córdoba Ciencia.

REFERENCES

Alcaino G. 1975, A&AS, 21, 15
Alcaino G. 1977a, A&AS, 29, 397

Alcaino G. 1977b, A&AS, 29, 383
Armandroff T. E., Zinn R. 1988, AJ, 96, 92
Arp H. 1955, AJ, 60, 317
Buonanno R., Buscema G., Corsi C. E., Iannicola G., Fusi Pecci F. 1983, A&AS, 51, 83
Caldwell S. P., Dickens R. J. 1988, MNRAS, 234, 87
Canterna R. 1976, AJ, 81, 228
Carretta E., Gratton R. G. 1997, A&A, 121, 95 (CG97)
Clariá J. J., Lapasset E. 1985, MNRAS, 214, 229
Clark J. P. A., McClure R. D. 1979, PASP, 91, 507
Cudworth K. M. 1976, AJ, 81, 519
Cudworth K. M. 1986, AJ, 92, 348
Cudworth K. M., Rausher E. A. 1987, AJ, 93, 856
Da Costa G. S., Armandroff T. E. 1990, AJ, 100, 1623
Davidge T. J., Harris W. E. 1997, ApJ, 475, 584
Dean J. F., Warren P. R., Cousins A. W. J. 1978, MNRAS, 183, 569.
Geisler D. 1984, PASP, 96, 723
Geisler D. 1986a, PASP, 98, 762
Geisler D. 1986b, PASP, 98, 847
Geisler D. 1990, PASP, 102, 344
Geisler D., Clariá J. J., Minniti D. 1991, AJ, 102, 1836 (GCM)
Geisler D., Clariá J. J., Minniti D. 1992a, AJ, 104, 1892
Geisler D., Lee M.G., Kim E. 1996, AJ, 111, 1529
Geisler D., Minniti D., Clariá J. J. 1992b, AJ, 104, 627
Geisler D., Sarajedini A. 1999, AJ, 117, 308 (GS)
Harris W.E. 2003, *Catalog of Parameters for the Milky Way Globular Clusters: the Database*, www.physics.mcmaster.ca/resources/globular.html
Harris W. E. 1996, AJ, 112, 1487
Harris W. E., Canterna R. 1979, AJ, 84, 1750
Kraft R. P., Ivans I. I. 2003, PASP, 115, 143
Minniti D., Coyne G., Clariá J. J. 1992, AJ, 103, 871
Minniti D., Geisler D., Peterson R. C., Clariá J. J. 1993, ApJ, 413, 548
Nelles B., Seggewiss W. 1984, A&A, 139, 79
Richter P., Hilker M., Richtler T. 1999, A&A, 350, 476
Rutledge G. A., Hesser J. E., Stetson P. B. 1997, PASP, 109, 907
Sandage A. 1970, ApJ, 162, 841
Shethrone M. D., Keane M. J. 2000, AJ, 119, 840
Straižys V. 1977, *Multicolor Stellar Photometry*, Mokslas Publishers, Vilnius, Lithuania
Straižys V. 1992, *Multicolor Stellar Photometry*, Pachart Publishing House, Tucson, Arizona
Straižys V., Zdanavičius K. 1965, Bull. Vilnius Obs., No. 14, 3
Zinn R. 1985, ApJ, 293, 424 (Z85)
Zinn R., West M.J. 1984, ApJS, 55, 45